Distribution of Gravity Wave Parameters over Eureka, Nunavut using the All Sky Imager

Chris Vail[1] and W. Ward[1]

1. Department of Physics, University of New Brunswick, Fredericton, Canada

Contact: c.w.vail@unb.ca

Introduction

The goal of research project is to develop a reliable automated technique in detecting gravity waves and their parameters from an All Sky Imager. The instrument being used is the PEARL (Polar Environment Atmospheric Research Laboratory) All Sky Imager (PASI), located in the high arctic at Eureka, Nunavut, Canada (80N 86W). PASI has been operating at PEARL since November 2007 and an automated technique to determine if gravity waves are present would allow for a good understanding of the climatology and dynamics events that can occur during the winter seasons.

Instrument

PASI is a CCD imaging system with six different narrow band interference filters. The filters used for the analysis on this poster are: sodium (at 589.3 nm), atomic oxygen green line (at 557.7nm) and hydroxyl (at 720-910nm notched at 865nm to mask molecular oxygen). The filters isolate emissions occurring at the following heights in the atmosphere: the hydroxyl emission occurs around 87km, the atomic oxygen green line emission occurs around 97km and the sodium emission occurs around 90km.

Picture of the PASI in 2007

Example of images that the PASI captures

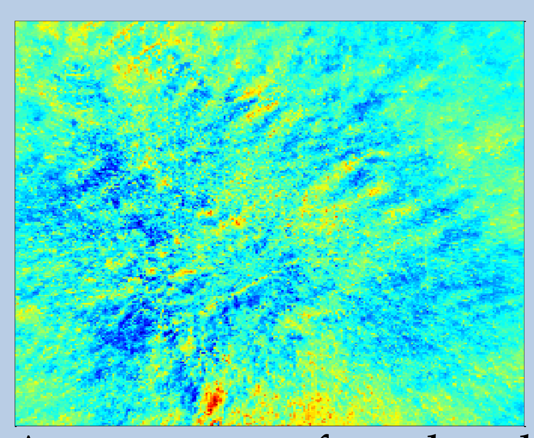

A wave event found and cleaned up from PASI

Analysis

The steps outlined to the side are implemented in order to determine the presence of gravity waves. In order to determine wave parameters , a Fourier Transform is used to identify the wavelength, direction and phase. The vertical wavelength is determined by identifying nearby multiple emissions and the particular wave in them and determining how the wave has moved between the three emissions. The waves are filtered according to the criteria: $\lambda_h > 10km, \lambda_m > 7\ km, \omega_{period} < 2\ hours, \Omega < N$

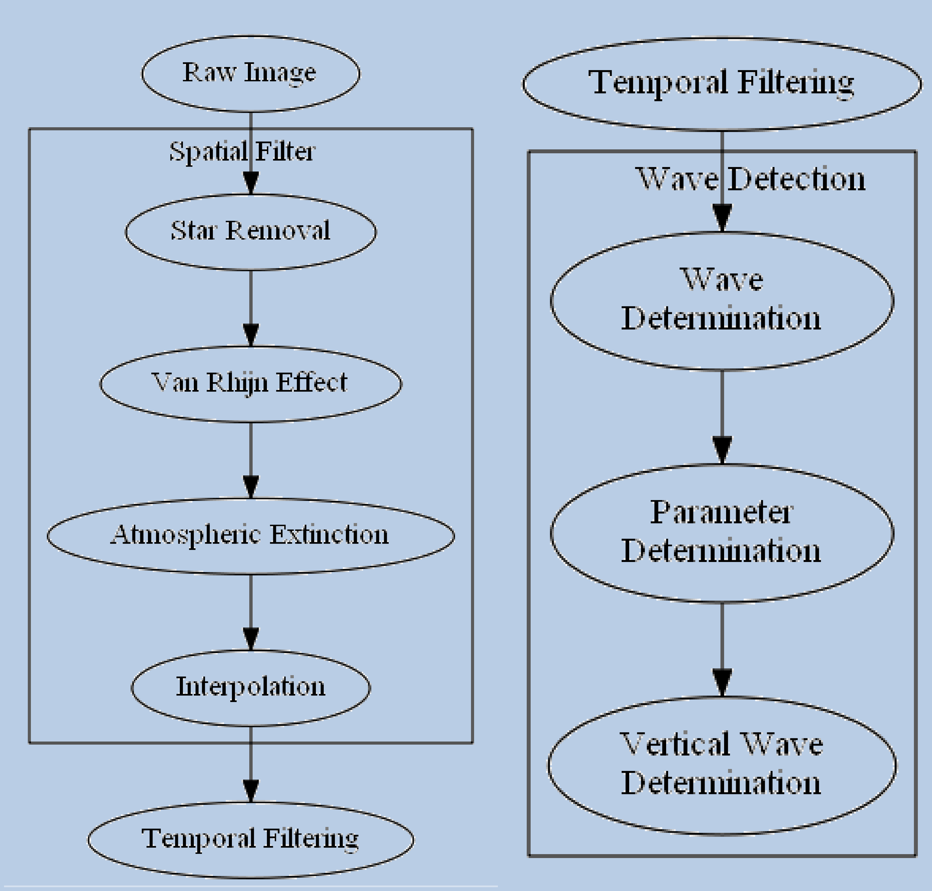

Data Present

During the observational seasons, there can be different events that lead to same of the images to be rejected for this analysis. Some of these events include the moon being present in the sky, instrument stopped working, power outage.

The plots below show the intensity seen at the zenith of the instrument from 1 November to 15 March during the 2008-2009, 2009-2010 and the 2012-2013 seasons.

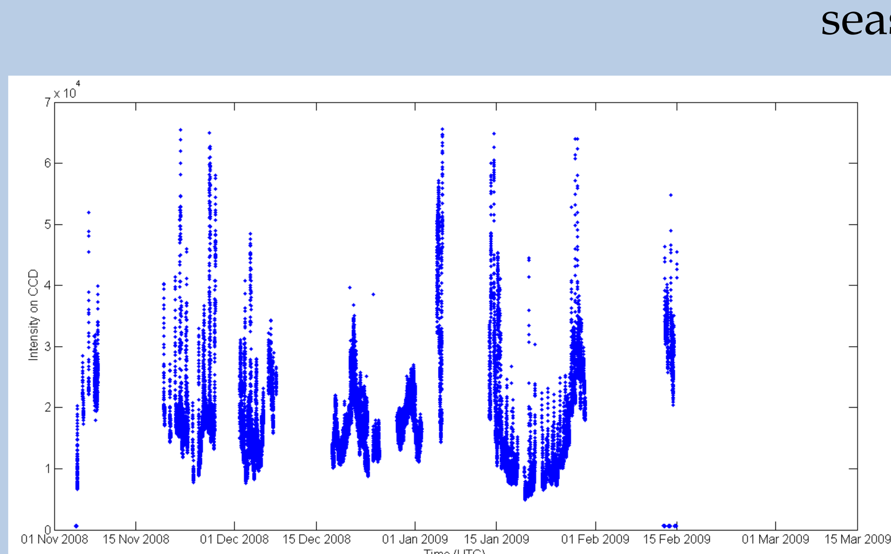

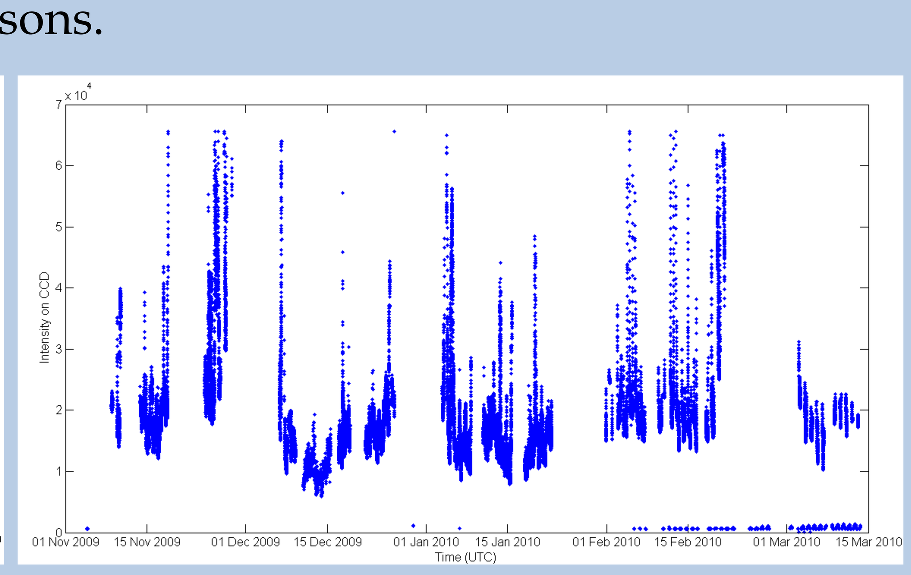

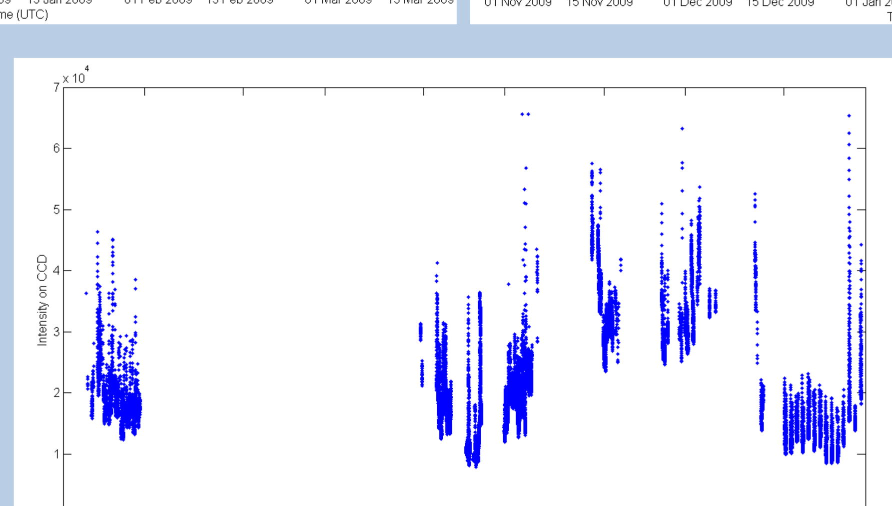

Results

After running this analysis for a season, we can track the change on a daily, monthly and seasonal basis and identify patterns in the wave parameters. The seasonal changes between 2008-2009, 2009-2010 Season and 2012-2013 seasons are below.

Seasonal Results for 2008-2009 Season

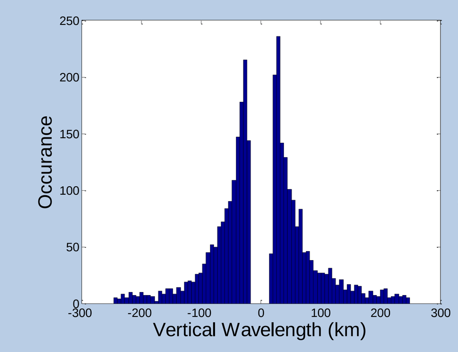

Histogram of Vertical Wavelength

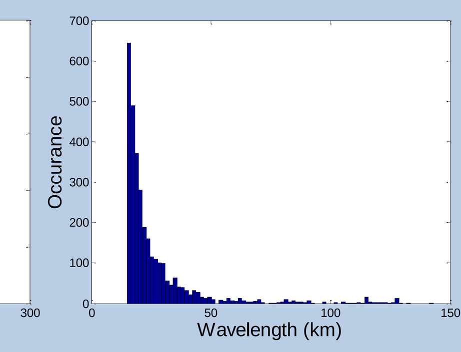

Histogram of Horizontal Wavelength

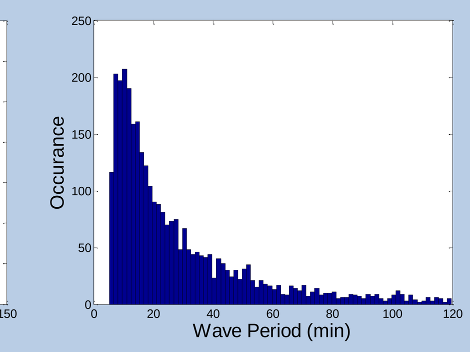

Histogram of Observed Period

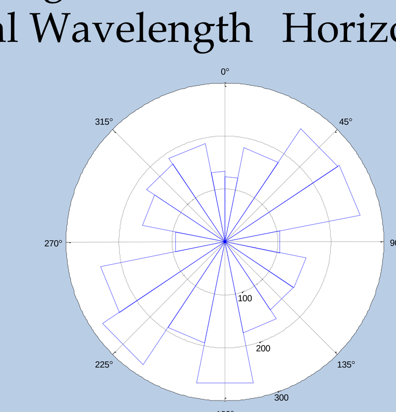

Wave Direction

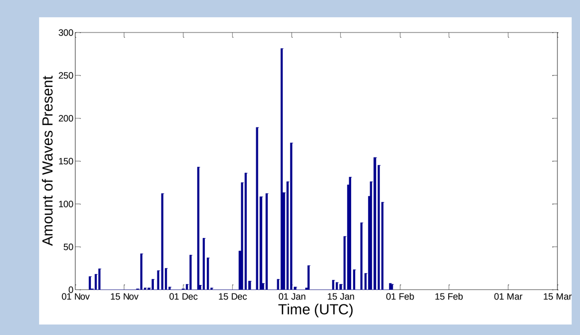

Amount of Waves seen over the Season

Seasonal Results for 2009-2010 Season

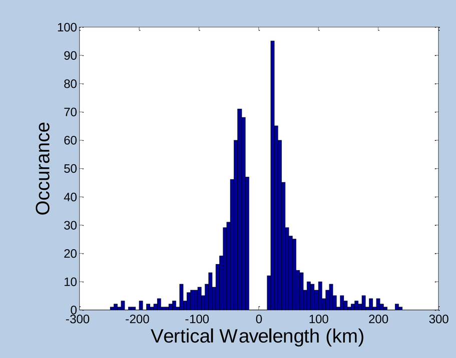

Histogram of Vertical Wavelength

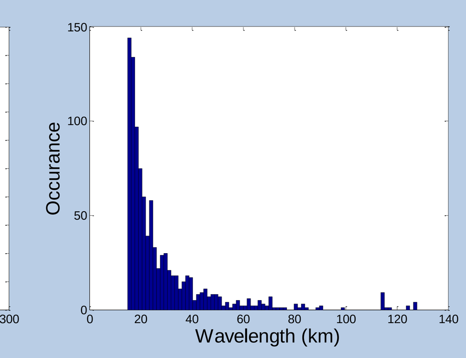

Histogram of Horizontal Wavelength

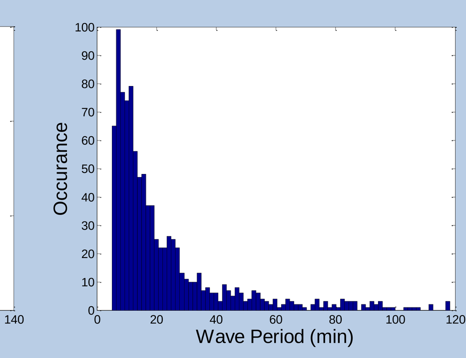

Histogram of Observed Period

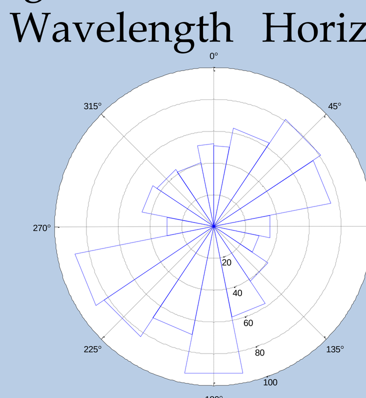

Wave Direction

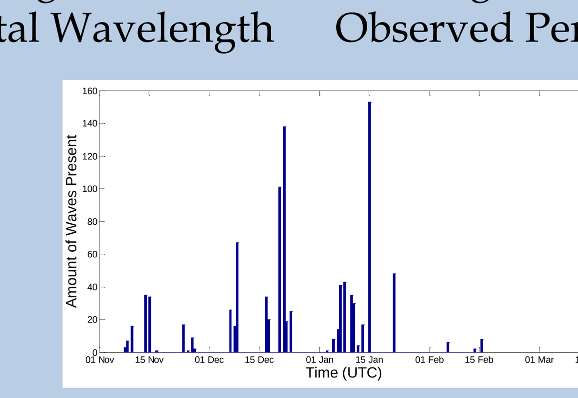

Amount of Waves seen over the Season

Seasonal Results for 2012-2013 Season

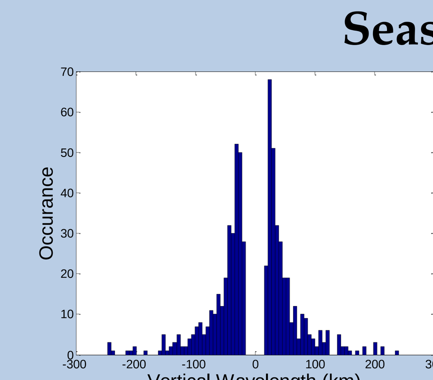

Histogram of Vertical Wavelength

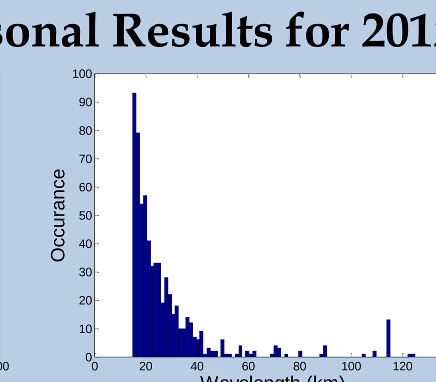

Histogram of Horizontal Wavelength

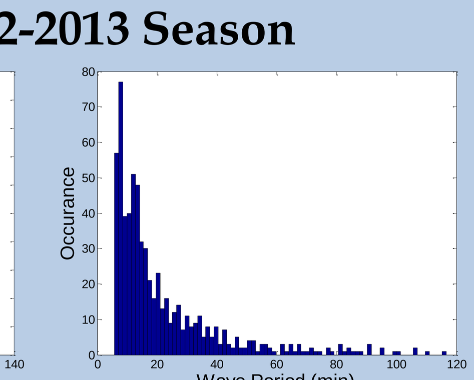

Histogram of Observed Period

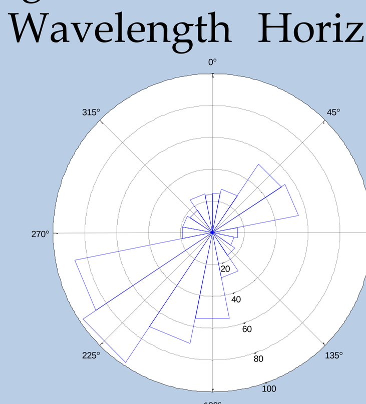

Wave Direction

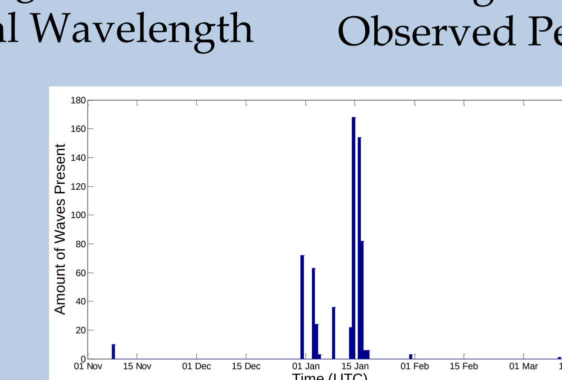

Amount of Waves seen over the Season

Conclusion

There are similarities between the three different seasons of data presented. Most of the waves observed during the observational season tend to occur mid to late January and waves tend to travel in a ENE or WSW direction.

A common feature in every season is that there are more waves with a horizontal wavelength less than 20km than any other wavelength combined and that the smallest vertical wavelength is around 15km.

References

Suzuki S., Shiokawa K., Otsuka Y., Ogawa T., Kubota M., Tsutsumi M., Nakamura T., and Fritts D.C. (2007) Gravity wave momentum flux in the upper mesosphere derived from OH airglow imaging measurements, Earth Planet Science, **59**, 421-428.

Tang, J., Farzad K., Franke S., Liu A., Swenson G. (2005) Estimation of gravity wave momentum flux with Spectroscopic imaging, IEEE Transactions on geoscience and remote sensing, **43**, 103-109

Suzuki S.,Shiokawa K., Hosokawa K., Nakamura K., Hocking W. (2009) Statistical characteristics of polar cap mesospheric gravity waves observed by an all-sky airglow imager at Resolute Bay, Canada, Journal of Geophysical Research, **114**,

Acknowledgement

Funding from NSERC CREATE, CFI, CSA